Journal of Imaging Science and Technology® 51(4): 1–XXXX, 2007.

Improved B-Spline Contour Fitting Using Genetic Algorithm for the Segmentation of Dental Computerized Tomography Image Sequences

Xiaoling Wu, Hui Gao, Hoon Heo, Oksam Chae, Jinsung Cho, Sungyoung Lee and Young-Koo Lee
Department of Computer Engineering, Kyunghee University, 1 Seochun-ri, Kiheung-eup, Yongin-si, Kyunggi-do, 449-701, South Korea
E-mail: xiaoling@oslab.khu.ac.kr, gaohui1977@hotmail.com, {hhoon,oschae,chojs,yklee}@khu.ac.kr, sylee@oslab.khu.ac.kr

Abstract. *In the dental field, 3D tooth modeling, in which each tooth can be manipulated individually, is an essential component of the simulation of orthodontic surgery and treatment. However, in dental computerized tomography slices teeth are located closely together or inside alveolar bone having an intensity similar to that of teeth. This makes it difficult to individually segment a tooth before building its 3D model. Conventional methods such as the global threshold and snake algorithms fail to accurately extract the boundary of each tooth. In this paper, we present an improved contour extraction algorithm based on B-spline contour fitting using genetic algorithm. We propose a new fitting function incorporating the gradient direction information on the fitting contour to prevent it from invading the areas of other teeth or alveolar bone. Furthermore, to speed up the convergence to the best solution we use a novel adaptive probability for crossover and mutation in the evolutionary program of the genetic algorithm. Segmentation results for real dental images demonstrate that our method can accurately determine the boundary for individual teeth as well as its 3D model while other methods fail. Independent manipulation of each tooth model demonstrates the practical usage of our method. © 2007 Society for Imaging Science and Technology.*
[DOI: XXXX]

INTRODUCTION

The accurate 3D modeling of the mandible and the simulation of tooth movement play an important role in preoperative planning for dental and maxillofacial surgery. The 3D reconstruction of the teeth can be used in virtual reality based training for orthodontics students and for preoperatory assessment by dental surgeons. For 3D modeling tooth segmentation to extract the individual contour of a tooth is of critical importance. Automated tooth segmentation methods from 3D digitized images have been researched for the measurement and simulation of orthodontic procedures.[1] These methods provide interstices along with their locations and orientations between the teeth for segmentation result. However, it does not give individual tooth contour information which manifests more details that are helpful in dental study. A thresholding method, used in the existing segmentation and reconstruction systems, is known to be efficient for automatic hard tissue segmentation.[2,3] Some morphological filtering methods are used for creating intermediary slices by interpolation for modeling teeth in 3D.[4] The morphological operations are also combined with the thresholding method for dental segmentation in x-ray films.[2] However, neither the thresholding method nor the morphological filtering method is suitable for separating individual tooth regions using tooth computerized tomography (CT) slices, because some teeth touch each other and some are located inside of alveolar bone with a CT slice intensity profile similar to teeth.[5] A modified watershed algorithm was suggested to create closed-loop contours of teeth while alleviating the over-segmentation problem of the watershed algorithm.[5] Although this reduces the number of regions significantly, it still produces many irrelevant basins that make it difficult to define an accurate tooth contour. A seed-growing segmentation algorithm[6] was suggested based on B-spline fitting for arbitrary shape segmentation in sequential images. The best contour of an object is determined by fitting the initial contour passed by previous frame to the edges detected in the current frame. For the fitting operation, the objective function defined by the sum of distances between the initial contour and the object edges is used. For this algorithm to work properly, the complete object boundary should be extracted by global thresholding and the object should be located apart from other objects. If other objects are located nearby as in the case of the tooth CT image, the shape of the initial contour should be very close to the actual object contour to prevent being fitted to the boundaries of the nearby objects.

Many snake algorithms have been proposed for medical image analysis applications.[7–10] However, in the CT image sequence where objects are closely located, the classical snake algorithms have not yet been successful due to difficulties in initialization and the existence of multiple extrema. It is only successful when it is initialized close to the structure of interest and there is no object which has similar intensity values to those of interest.[7] The snake models for object boundary detection search for an optimal contour that minimizes (or maximizes) an objective function. The objective function generally consists of the internal energy representing the properties of a contour shape and the external potential energy depending on the image force. The final shape of the contour is influenced by how these two energy terms are represented. However, many snakes tend to shrink when its external energy is relatively small due to the lack of image

forces.[7] Some snakes also suffer from the limited flexibility of representing the contour shape and a large number of derivative terms in their internal energy representation. A B-spline based snake has been developed as a B-spline snake and B-snake to enhance the geometric flexibility and optimization speed by means of a small number of control points instead of snaxels.[11,12] B-spline snake controls contour shapes by a stiffening parameter as well as its control points, and detects object boundaries in noisy environments by using gradient magnitude information instead of edge information. This algorithm introduces a stiffening factor to the B-spline function[13] that varies the spacing between the spline knots and the number of sampled points used during the evaluation of the objective function. In addition, the factor controls the smoothness of curve and reduces the computation of the cost function. Although the algorithm was proposed to extract the contour of a deformable object in a single image, it can be applied to the tooth segmentation in CT slices. However, in tooth CT data, the algorithm may cause the contour of a tooth to expand to include contours of nearby teeth and alveolar bone, or it may cause the contour to be contracted to a small region.

A B-spline fitting algorithm employing a genetic algorithm (GA) was used to overcome local extrema indwelling in the vicinity of an object of interest.[14–17] In this case, it was shown that the GA does not require exhaustive search while avoiding high-order derivatives for curve fitting or matching problems.[18,19] However, the conventional GA-based B-spline fitting still suffers from the influence of other objects and often fails to extract the object boundary from the image sequences when similar objects are adjacent to each other.

In this paper, we propose an improved B-spline contour fitting algorithm using a GA to generate a smooth and accurate tooth boundary for the 3D reconstruction of a tooth model. We devise a new B-spline fitting function by incorporating the gradient direction information on the fitting contours to search the tooth boundary while preventing it from being fitted to neighboring spurious edges. We also present an evolution method to accelerate the search speed by means of automatic and dynamic determination of GA probabilities for crossover and mutation. Experimental results show that our method can successfully extract the individual tooth boundary, compared with other methods which fail to do so.

BACKGROUND

Dental CT images have the following two distinct characteristics: (1) An individual tooth often appears with neighboring hard tissues such as other teeth and alveolar bone, and (2) these neighboring hard tissues have the same or similar intensity values to the tooth of interest. Thus, the fixed threshold value for each tooth in each slice is not effective as shown in Figure 1. When we try to obtain a tooth region by thresholding method, the lower and upper limits of a threshold value can be displayed at each slice for a given tooth by the two curves in Fig. 1. Any threshold value within the limit produces the tooth region with the accuracy better than

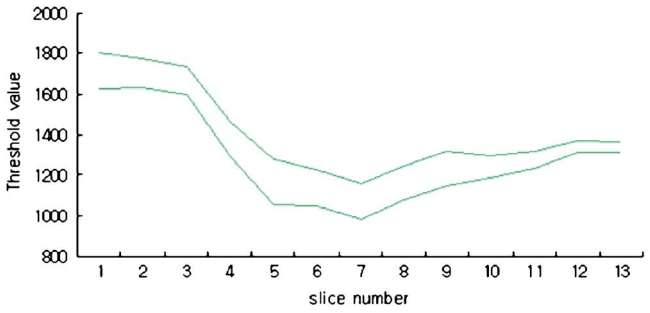

Figure 1. Threshold values for a certain tooth computed at different slices by manual.

90%. It shows us that individual segmentation method is required for each tooth in each slice.

There are many segmentation methods, each of which have their own limitations in separating individual tooth regions on CT images.[3–6] An optimal thresholding scheme[20] can be attempted by taking advantage of the fact that the shape and intensity of each tooth changes gradually through the CT image slices.

However, even if an optimal threshold is determined for every slice, the result of the segmentation is found unsatisfactory because of neighboring hard tissue. For the 3D reconstruction of an individual tooth model, the tooth boundary needs to be defined more precisely.

B-Spline Contour Fitting

The B-spline curve has attractive properties for the representation of an object contour with arbitrary shape. They are also suitable for the curve fitting process and are summarized as follows.

- An object of any shape, including those subsuming angular points, can be represented by a set of control points, a knot sequence, and a basis function. The shape of the contour can be adjusted by simply repositioning the control points in many fitting problems where the knot sequence and basis function can be fixed.
- Little else remains to be different in the shape of the contour by deducting the number of control points within some tolerable limit for the purpose of reducing information needed for fitting process. This allows the fitting process to be faster with fewer variables over which to optimize.

We choose the uniform cubic closed B-spline curve, shown as follows in Eqs. (1) and (2), to describe the object contours in the image:

$$\mathbf{r}(s) = \begin{bmatrix} r_x(s) \\ r_y(s) \end{bmatrix} = \begin{bmatrix} \sum_{i=0}^{n-1} x_i B_0(s-i) \\ \sum_{i=0}^{n-1} y_i B_0(s-i) \end{bmatrix}, \quad (1)$$

$$B_0(s) = \begin{cases} |s|^3/2 - s^2 + 2/3 & \text{if } t_0 \le |s| < t_1, \\ (2-|s|)^3/6 & \text{if } t_1 \le |s| < t_2, \\ 0 & \text{otherwise.} \end{cases} \quad (2)$$

In the equations, $\mathbf{r}(s)$ represents the coordinate of a contour pixel at a specific value of parameter s and (x_i, y_i) represents coordinates of ith control point. The B-spline basis functions are translated copies of $B_0(s)$. In the case of tooth segmentation we use a closed uniform knot sequence, as $\{t_0, t_1, \ldots, t_n\} = \{0, 1, \ldots, n\}$ and $t_0 = t_n$ where n is the total number of the control points.

The B-spline fitting function f is represented in Eq. (3) (Ref. 11) as follows:

$$f = \sum_{k=0}^{M-1} |\nabla I[\mathbf{r}(s_k)]|, \quad (3)$$

where M is the total number of contour points. The fitting function is maximized when the contour conforms to the object boundary. The B-spline fitting function makes use of only external force computed based on the gradient magnitude on the contour. The smoothness constraint is implicitly represented by the B-spline itself.

B-spline Contour Fitting using Genetic Algorithm

The genetic algorithm is a probabilistic technique for searching for an optimal solution. The optimal solution is described by a vector, called a "chromosome," which can be obtained by maximizing a fitting function. Hence the definition of the fitting function significantly affects the solution state. A sequence of evolutionary operations is repeated for a chromosome to evolve to its final state. The end of the evolutionary operation is determined by checking the fitness values, which represent the goodness of each chromosome in the population.

A chromosome is a collection of genes, and a gene represents the control point of B-spline. Since the chromosome represents a complete contour and a gene uses the actual location of a control point, the search algorithm has neither ambiguity on the contour location nor potential bias to particular shapes. To reduce the size of a gene, we use the index value as a gene, instead of two coordinate values.[16,17] Composing a search area based on the indices provides a search area with arbitrary shape, where it is confined to search for the final position of the control point to be found out. This scheme of chromosome guarantees that gene information does not spread over the chromosome, which results in short length and order of schema.[16] Accordingly, there is a high probability to converge fast. A new generation is made through the sequence of evolutionary operations and, during the evolutionary processes, crossover and mutation steps affect the quality and speed of final solution significantly.

IMPROVED B-SPLINE CONTOUR FITTING USING GENETIC ALGORITHM

Fitting Function Based on Gradient Magnitude and Direction

The fitting function measures the fitness of the possible contour to the object boundary in the current slice. The fitness

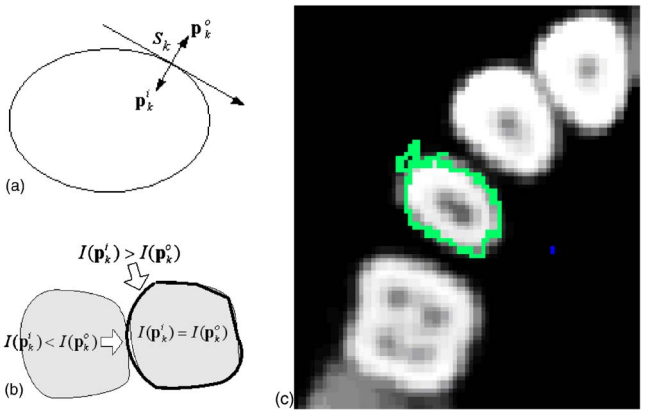

Figure 2. (a) Definition of inner and outer regions. (b) Illustration for fitting function—right object is of interest, with adjacent left object, and thick black curve is a fitting curve. (c) Twisted contour.

value is the basis for determining the termination of the evolutionary process and selecting elite chromosomes for mating pool generation. In the existing active contour models, the fitting function consists of the internal forces controlling the smoothness of the contour and the external force used for representing the object boundary information in the image.[7,12] One drawback of this representation is that it requires the determination of the weight values balancing these two components.

B-spline snake makes use of a simple fitting function with only external force computed based on the gradient magnitude on the contour. The internal force terms are replaced by using a stiffening parameter and implicit smoothness constraint of the B-spline representation of a contour. However, in the image data such as the tooth CT image slices, those fitting functions often generate the contour fitted to the boundary of nearby object. They also generate the contour contracted to a small region unless the stiffening parameter is set properly.

Note that the magnitude of the intensity difference may vary between the inside and outside of an object contour. However, if the relative intensity between two sides of a contour is maintained throughout the contour, the sign of the intensity difference made by two sides is inverted when the contour expands out to the boundary of another object. Hence, when fixing moving direction of parameter s along the curve, we are able to have knowledge of which side is inside (or outside) in advance. This enables us to know whether the contour is fitted to the object of interest or other adjacent objects. In this paper, the fitting function to be maximized is designed to take advantage of this property of the data. This gradient direction information allows the fitness function to penalize the portion of a contour fitted to the neighboring object.

To compute the fitness value for a possible solution (or chromosome), we first generate the contour points from the B-spline representation of the solution and trace the contour as shown in Figure 2(a). At the kth contour point $\mathbf{r}(s_k)$, a unit normal vector $\mathbf{n}(s_k)$ is computed. Next, the inner region and outer region pixel location $\mathbf{p}_k^i$ and $\mathbf{p}_k^o$, respectively, are

identified by using $\mathbf{n}(s_k)$ computed at the kth point $\mathbf{r}(s_k)$ according to

$$\mathbf{p}_k^o = \mathbf{r}(s_k) + \mathbf{n}(s_k) \tag{4}$$

and

$$\mathbf{p}_k^i = \mathbf{r}(s_k) - \mathbf{n}(s_k). \tag{5}$$

Then, the fitness value is determined based on gradient magnitude and direction information, ∇_k, at each contour point according to

$$f = \sum_{k=0}^{M-1} (\nabla_k - \alpha_k), \tag{6}$$

where

$$\nabla_k = \begin{cases} |\nabla I[\mathbf{r}(s_k)]| & \text{if } I(\mathbf{p}_k^i) - I(\mathbf{p}_k^o) > 0, \\ -|\nabla I[\mathbf{r}(s_k)]| & \text{if } I(\mathbf{p}_k^i) - I(\mathbf{p}_k^o) \le 0, \end{cases}$$

and

$$\alpha_k = \begin{cases} C, & \mathbf{r}(s_k) = \mathbf{r}(s_j) \\ 0, & \mathbf{r}(s_k) \neq \mathbf{r}(s_j) \end{cases}, \forall\, j \in \{0, 1, \ldots, M-1\} \wedge j \neq k.$$

$I(\mathbf{p}_k^i)$ and $I(\mathbf{p}_k^o)$ are intensity values of the inside and outside of the kth contour point, respectively. This equation is further illustrated by Fig. 2(b), where some portion of the contour attaches to another object and in this portion $I(\mathbf{p}_k^i) < I(\mathbf{p}_k^o)$, so we assign the negative gradient magnitude to penalize the fitness value. The figure also shows that in other portions the contour correctly conforms to the tooth boundary and in these portions $I(\mathbf{p}_k^i) > I(\mathbf{p}_k^o)$, so we assign the positive gradient magnitude to the fitness value. Note that when there is no difference of gradient direction, which may happen if inner and outer pixel values are identical, then $I(\mathbf{p}_k^i) = I(\mathbf{p}_k^o)$. This aims at preventing the contour from being misfitted when the contour lies inside an object region having uniform intensity values, such as the inside region of a tooth.

A constant-valued penalty C is deducted from the fitness value when the contour is twisted as shown in Fig. 2(c). Our experimental results showed that setting the penalty too high hindered searching the contour maximizing the sum of gradient magnitudes. The proposed fitting method yields the best performance when C is set to around 0.1% of the sum of gradient magnitudes.

Improved Adaptive Evolutionary Operations

The evolutionary process generates a new population of possible solutions through the following three genetic operators: reproduction (or selection), crossover, and mutation. The selection operation constructs the mating pool from the current population for the crossover operation. The results presented here use a tournament selection scheme.[16] The crossover operation generates two child chromosomes by swapping genes between the two parent chromosomes. In this paper we present one point cutting scheme by improved adaptive crossover probability. We also use an adaptive mutation probability scheme for our evolutionary process.

The conventional GA generally uses fixed crossover and mutation probabilities. Adaptive genetic algorithm[21] (AGA) was proposed by Srinivas et al. that uses variable crossover and mutation probabilities that are determined automatically based on fitness values during fitting process for fast convergence rate. The probabilities for evolution are, therefore, no longer required to be set to constants. At the beginning stage of the fitting process, we consider all the possibilities of control point locations in the search area. As the process goes on, we obtain the evolutionary probabilities such that the possible solution near the optimal solution quickly converges to the actual solution. In AGA,[21] the crossover probability is adaptively determined depending on the fitness value f, according to

$$p_c = \begin{cases} k_1 \dfrac{f_{\text{best}} - f}{f_{\text{best}} - f_{\text{avg}}}, & f \ge f_{\text{avg}}, \\ k_2, & f < f_{\text{avg}}, \end{cases} \tag{7}$$

where f_{best} and f_{avg} are the best and average fitness values in the mating pool, respectively, and k_1 and k_2 are constants and set to 1.0. Hence, if $f = f_{\text{best}}$ when $f \ge f_{\text{avg}}$, f is preserved, although the value of k_1 ensures high occurrence of crossover. If $f < f_{\text{avg}}$, crossover is operated without exceptions, since its corresponding chromosome has low fitness value.

The mutation operation is also implemented by using the mutation probability p_m as follows:

$$p_m = \begin{cases} k_3 \dfrac{f_{\text{best}} - f}{f_{\text{best}} - f_{\text{avg}}}, & f \ge f_{\text{avg}}, \\ k_4, & f < f_{\text{avg}}, \end{cases} \tag{8}$$

where k_3 and k_4 are constants set to 0.5. As in the case of crossover, the mutation operation does not affect the chromosome with the best fitness value. However if $f \le f_{\text{avg}}$ its mutation operation takes place with the most ambiguity since $k_3 = 0.5$.

In this paper we propose an improved adaptive crossover probability. To maintain the solution with high fitness value, we generate a random number p_r and consider the relationship of p_r with p_{c1} and p_{c2}, where p_{c1} and p_{c2} denote crossover probabilities generated from two parent chromosomes, father chromosome and mother chromosome respectively. When two parent chromosomes are selected, two children are generated as follows.

(1) Generate a random number p_r between 0 and 1 to determine the adaptive crossover probability, generate a random number p_l between 0 and 1 to determine the crossing site, and generate a random number p_s between 0 and 1 to determine which side of the crossing site the portion of the chromosome should exchange with the corresponding portion of its mate.

(2) Replace f in Eq. (7) by the fitness value of each parent for computing the crossover probabilities, p_{c1} and p_{c2}.
(3) If $p_r > p_{c1}$ and $p_r > p_{c2}$, put the two parents to the next generation without change.
(4) If p_r is between p_{c1} and p_{c2}, thus $p_{c1} \geq p_{c2}$ and $p_s < 0.5$ then the left portion of the father chromosome should be exchanged with the corresponding portion of the mother chromosome to generate one child and put mother chromosome directly to the generation as another child. If $p_s \geq 0.5$ then the right portion from the father chromosome should be exchanged to generate one child and another child is a copy of the mother chromosome. Similarly if $p_{c1} < p_{c2}$ then the mother chromosome should be changed and put to the next generation while the father chromosome is put to the next generation without any change. In addition, the crossover scheme is determined by the value of p_s.
(5) If p_r is less than both p_{c1} and p_{c2}, generate two child chromosomes as the normal crossover method does.

In the proposed operation, the chromosomes with high fitness values can survive until a new chromosome with higher fitness is created. It supports rapid searching for an optimal solution by taking advantage of the crossover scheme swapping either side to the crossing site.

EXPERIMENTAL EVALUATION

We tested the proposed contour segmentation with two kinds of sets of data: synthetic images and two sets of real dental CT image sequences with a slice thickness of 0.67mm and 1mm and x-y resolution of 512×512. Visual C++ with DICOM libraries[22] for reading 16-bit CT images and the 3D graphics library OpenGL were used as tools to implement the proposed algorithm. CT images are saved in DICOM format, an international standard for medical images, after acquisition through the commercially available Shimadzu Ltd. SCT-7800 CT scanner. The test data were prepared to reveal the capability of the proposed algorithm in finding an accurate boundary among many similar objects nearby. We compared the proposed algorithm with the existing B-spline snake algorithm that uses the gradient magnitude based external force in the fitting function.[11]

First, we applied these algorithms to a synthetic image similar to a tooth surrounded by alveolar bone. To generate the results, we constructed a B-spline contour with 8 control points and selected 20 initial chromosomes for each 40×40 window. For the following examples of B-spline snake the stiffening parameter is set to 2. As shown in Figure 3, the proposed algorithm extracts an accurate object boundary while the existing B-spline snake fails.

We also applied the two algorithms to real CT image sequences where an individual tooth often appears with neighboring hard tissues such as other teeth and alveolar bone. If too many control points are used for a contour, it reduces the smoothing effect on the curve and consequently generates twisted parts of contour as shown in Figure 4. Figure 5 shows part of test results using different set of slices, which have lower resolution. Since the test image is small, a 10×10 search area suffices for a control point.

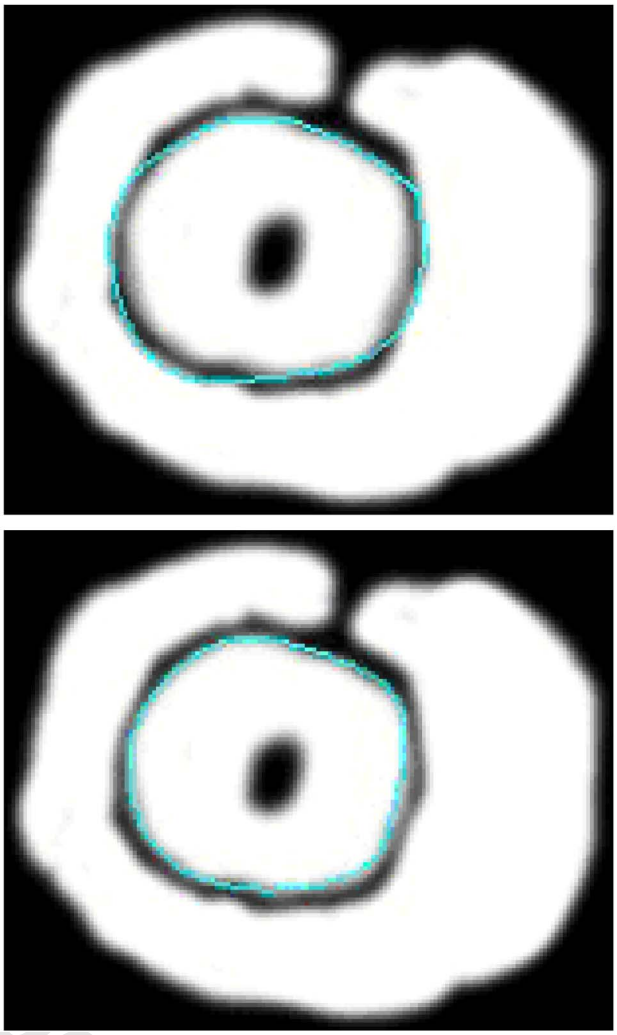

Figure 3. Contours extracted from the synthetic data (number of control points $CP=8$). (a) By B-spline snake method. (b) By the proposed method.

As shown in Fig. 5, an individual tooth often appears with neighboring hard tissues such as other teeth and alveolar bone, and the proposed algorithm produces better results than B-spline snake. The difference in the results stems from the fitting function.

Part of the segmentation results of slice sequences is shown in Figure 6 and those of a molar having a more complicated shape are shown in Figure 7. In Fig. 6, the figures at the far left side show the results of teeth initialization for the first slice by applying a proper threshold to each tooth interactively. As the segmentation is performed slice by slice, in contrast with the results of proposed method, malfitting error contained in the results of the existing method increases.

Table I lists part of the numerical results of the segmentation. N is the number of slices over which each tooth spans. FPE (false positive error) is the percent of area re-

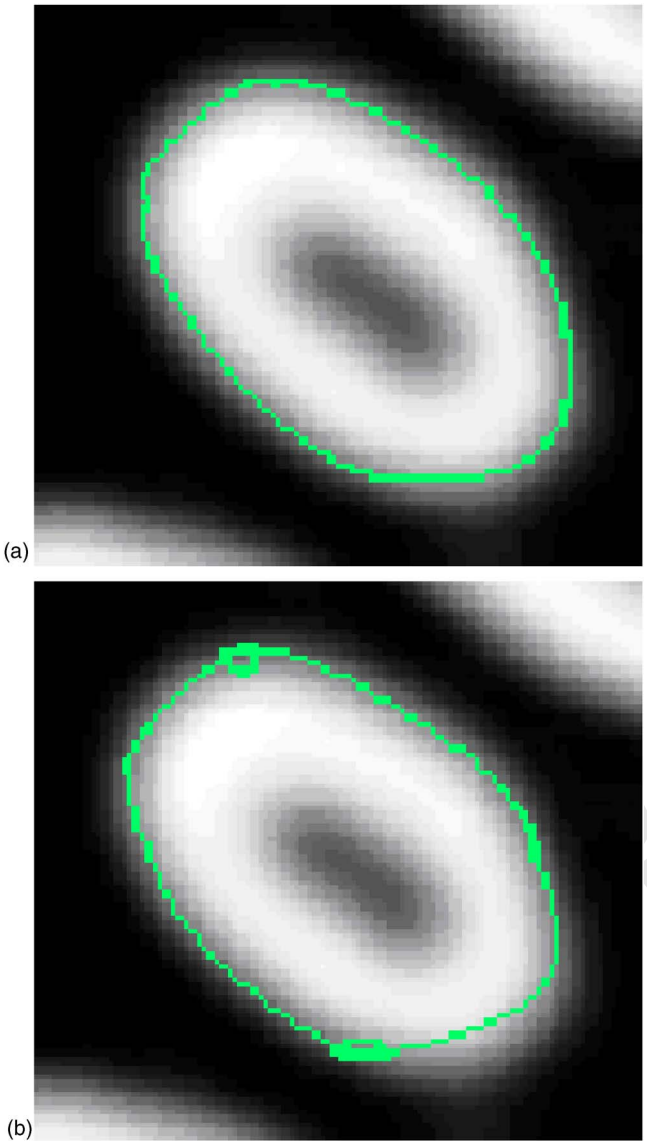

Figure 4. Tooth contours extracted from CT image (CP=16). (a) By the proposed method. (b) By B-spline snake.

ported as a tooth by the algorithm, but not by manual segmentation. FNE (false negative error) is the percent of area reported by manual segmentation, but not by the algorithm. Similarity and dissimilarity indices,[23,10] which show the amount of agreement and disagreement, S_{agr} and S_{dis}, respectively, between the algorithm area A_{alg} and the manual segmentation area A_{man}, are computed according to

$$S_{agr} = 2\frac{A_{man} \cap A_{alg}}{A_{man} + A_{alg}}, \tag{9}$$

$$S_{dis} = 2\frac{A_{man} \cup A_{alg} - A_{man} \cap A_{alg}}{A_{man} + A_{alg}}. \tag{10}$$

These indices are calculated for validation on N slices of each tooth. Averaged values of S_{agr} as well as its minimum and maximum values are shown in Table I, and we conclude

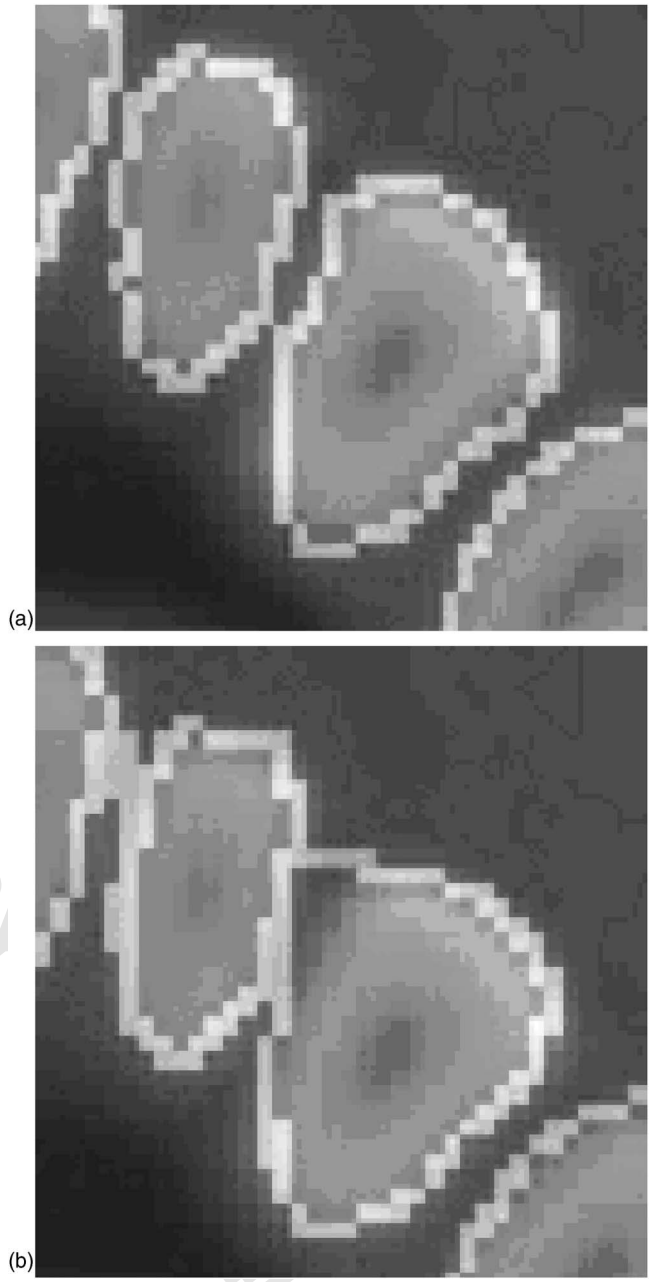

Figure 5. Tooth contours extracted from CT image sequence (CP=8). (a) By the proposed method. (b) By B-spline snake.

that the proposed method for segmentation isolates individual region of tooth successfully, in contrast with the results of B-spline snake shown in Table II.

The proposed fitting method is designed for the fast contour extraction by the improved crossover method which uses a random number for copying genes of a superior chromosome to an inferior one when the random number falls into the range of crossover probabilities of its parents, p_{c1} and p_{c2}. Furthermore, the proposed crossover method decides which part of crossing site will be exchanged between parent chromosomes. The decided part fosters chromosomes to be competent with a high fitness value. We implement two genetic B-spline fittings with existing crossover methods to analyze the performance of the proposed cross-

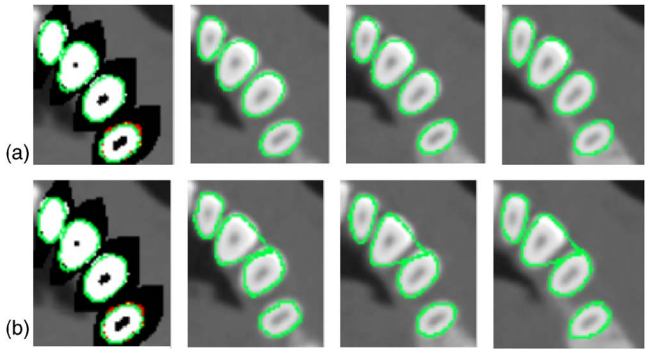

Figure 6. Tooth contours extracted from CT image sequence ($CP=16$). (a) By the proposed method. (b) By B-spline snake.

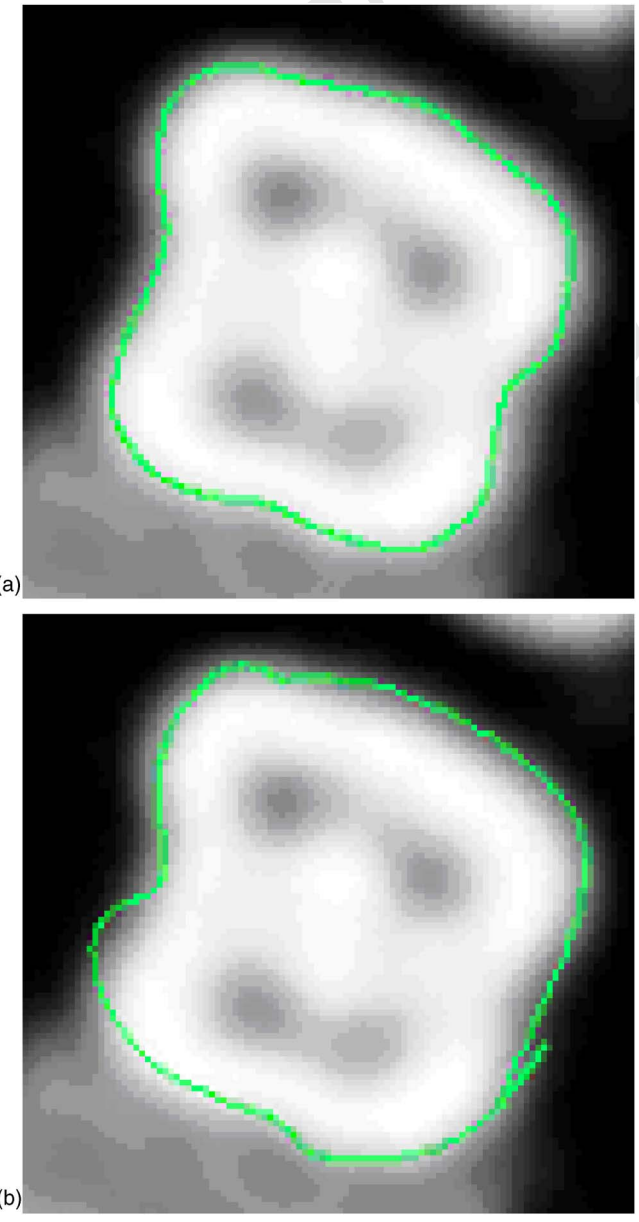

Figure 7. Extracted contours of molar ($CP=32$). (a) By the proposed method. (b) By B-spline snake.

Table I. Segmentation results for 8 teeth of the proposed method from the same scans of CT set.

Tooth	N	FPE[%]	FNE[%]	S_{agr}	S_{min}	S_{max}	S_{dis}
1	20	4.43	8.37	0.935	0.915	0.977	0.131
2	22	7.88	3.45	0.945	0.916	0.973	0.111
3	25	8.96	4.48	0.935	0.901	0.968	0.131
4	24	8.46	6.47	0.926	0.905	0.970	0.148
5	27	5.81	8.29	0.929	0.917	0.967	0.143
6	26	2.07	7.05	0.953	0.923	0.971	0.094
7	25	5.21	3.79	0.955	0.927	0.976	0.089
8	23	5.69	1.42	0.965	0.932	0.983	0.069

Table II. Segmentation results for 8 teeth of B-spline snake from the same scans of CT set.

Tooth	N	FPE[%]	FNE[%]	S_{agr}	S_{min}	S_{max}	S_{dis}
1	20	6.12	27.21	0.814	0.574	0.952	0.373
2	22	26.01	1.16	0.879	0.628	0.956	0.241
3	25	45.86	11.28	0.756	0.316	0.897	0.487
4	24	29.89	4.59	0.842	0.764	0.941	0.313
5	27	28.06	8.06	0.836	0.726	0.933	0.328
6	26	15.09	8.81	0.884	0.818	0.948	0.232
7	25	27.98	5.03	0.852	0.755	0.936	0.296
8	23	10.12	3.89	0.932	0.771	0.972	0.136

over. Both existing methods generate the initial population randomly, with uniform distribution, while using different crossover methods. "Method A" uses a fixed p_c of 0.75 and "Method B" uses AGA, which determines p_c adaptively. Figure 8 compares the convergence rate of the proposed crossover method with those of the existing methods in terms of the fitness value along chromosome generation. The figure shows that the proposed crossover method results in a better convergence rate than either method A or B. The proposed crossover method preserves the chromosomes with high fitness for fast convergence and the results shows it is effective to randomly select either side to crossing site for improved crossover operation.

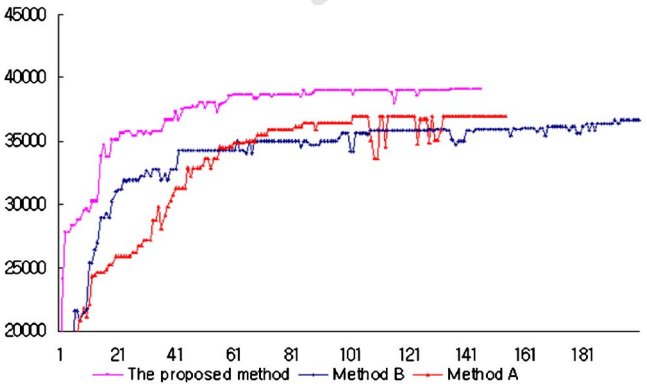

Figure 8. Comparison of convergence rates.

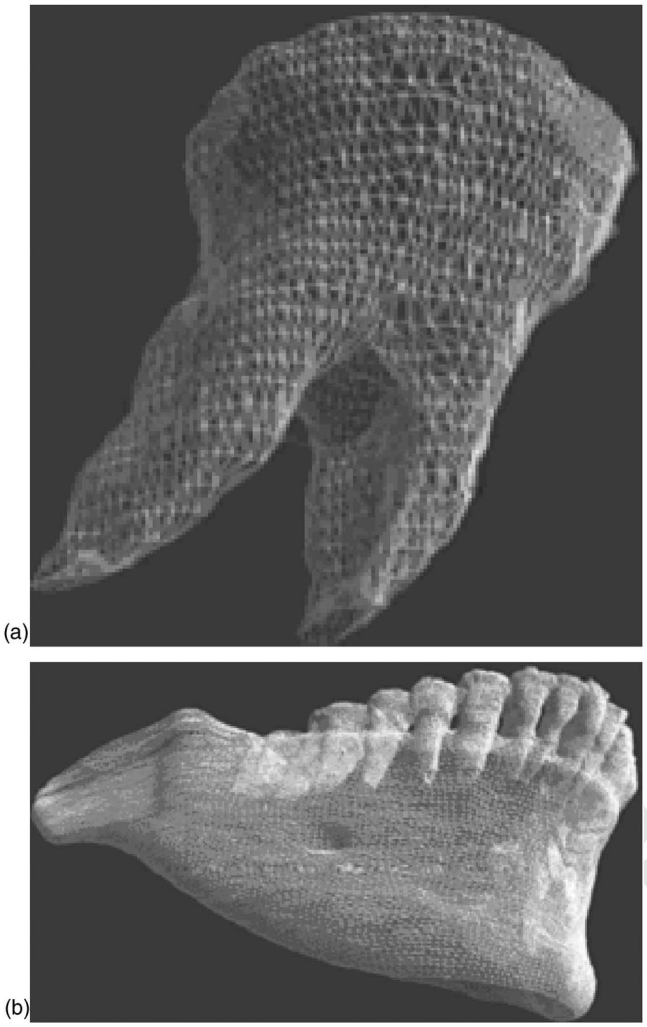

Figure 9. Wireframe models of tooth and mandible. (a) 3D reconstruction of tooth. (b) 3D reconstruction of mandible.

Individual segmentation of all teeth can be used to reconstruct a model of the mandible, as shown in Figures 9 and 10. Every tooth can be separated from the jaw for simulation of dental treatments.

CONCLUSIONS

In this paper, we presented the improved genetic B-spline curve fitting algorithm for extracting individual smooth tooth contours from CT slices while preventing the contour from being twisted. This enables us to obtain individual accurate contours of teeth by overcoming the problem of the contour of a tooth expanding out to other teeth boundaries in the fitting process. Furthermore, we also devised the crossover method which accelerates convergence rate by means of both conserving chromosomes with high fitness value and allowing exchange of either side of cross site. The test results show that the proposed segmentation algorithm successfully extracts a smooth tooth contour under specific conditions such as the existence of objects in close vicinity.

This paper also demonstrated the possibility of reconstruction of a 3D model in which each tooth was modeled and manipulated separately for the simulation of dental surgery. These anatomical 3D models can be used for facilitating diagnoses, pre-operative planning and prosthesis design. They will provide radiography of the mandible, an accurate mechanical model of the individual tooth and that of its root for endodontics and orthodontic operations. Hence the 3D reconstruction of the teeth can be used in virtual reality based training for orthodontics students and for preoperatory assessment by dental surgeons.

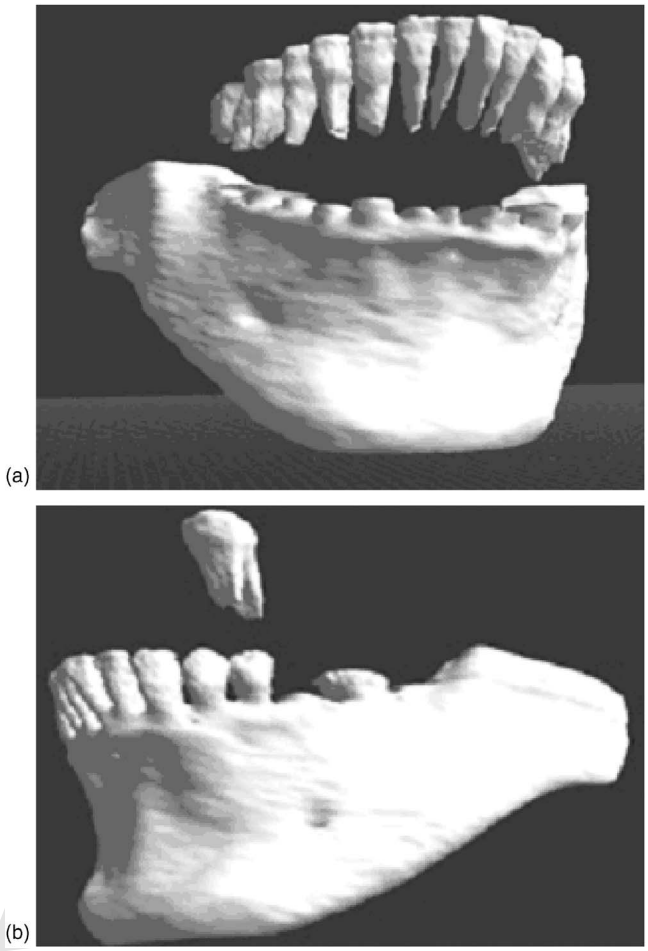

Figure 10. Manipulation of tooth. (a) Every tooth can be manipulated. (b) Simulation of having tooth out.

REFERENCES

[1] T. Kondo, S. H. Ong, and K. W. C. Foong, "Tooth segmentation of dental study models using range images", IEEE Trans. Med. Imaging **23**, 350–362 (2004).
[2] E. H. Said, D. E. M. Nassar, G. Fahmy, and H. H. Ammar, "Teeth segmentation in digitized dental X-ray films using mathematical morphology", IEEE Trans. Inf. Forensics Security **1**, 178–189 (2006).
[3] J. H. Ryu, H. S. Kim, and K. H. Lee, "Contour based algorithms for generating 3D CAD models from medical images", Int. J. Adv. Manuf. Technol. **24**, 112–119 (2004).
[4] A. G. Bors, L. Kechagias, and I. Pitas, "Binary Morphological Shape-Based Interpolation Applied to 3-D Tooth Reconstruction", IEEE Trans. Med. Imaging **21**, 100–108 (2002).
[5] G. Bohm, C. Knoll, V. G. Colomer, M. Alcaniz-Raya, and S. Albalat, "Three-dimensional segmentation of bone structures in CT images", Proc. SPIE **3661**, 277–286 (1999).
[6] S. Liu and W. Ma, "Seed-growing segmentation of 3D surfaces from CT-contour data", Computer-Aided Design **31**, 517–536 (1999).
[7] M. Kass, A. Witkin, and D. Terzopoulos, "Snakes: Active contour models", Int. J. Comput. Vis. **1**, 321–331 (1988).

[8] C. Han and W. S. Kerwin, "Detecting objects in image sequences using rule-based control in an active contour model", IEEE Trans. Biomed. Eng. **50**, 705–710 (2003).
[9] A. Klemencic, S. Kovacic, and F. Pernus, "Automated segmentation of muscle fiber images using active contour models", Cytometry **32**, 317–326 (1998).
[10] J. Klemencic, V. Valencic, and N. Pecaric, "Deformable contour based algorithm for segmentation of the hippocampus from MRI", in: Proc. 9th International Conference on Computer Analysis of Images and Patterns, Lect. Notes Comput. Sci. **2124**, 298–308 (2001).
[11] P. Brigger, J. Hoeg, and M. Unser, "B-Spline snakes: A flexible tool for parametric contour detection", IEEE Trans. Image Process. **9**, 1484–1496 (2000).
[12] S. Menet, P. Saint-Marc, and G. Medioni, "Active contour models: overview, implementation and applications. Systems", in *Proc. Man and Cybernetics*, (IEEE Press, Piscataway, NJ, 1990), pp. 194–199.
[13] G. Farin, *Curves and surfaces for CAGD*, 4th ed. (Academic Press, New York, 1996), pp. 141–168.
[14] M. Cerrolaza, W. Annicchiarico, and M. Martinez, "Optimization of 2D boundary element models using B-splines and genetic algorithms", in *Engineering Analysis with Boundary Elements* (Elsevier, Oxford, 2000), Vol. **24**, pp. 427–440.
[15] W. Annicchiarico and M. Cerrolaza, "Finite elements, genetic algorithms and B-splines: a combined technique for shape optimization", Finite Elem. Anal. Design **33**, 125–141 (1999).
[16] C. Ooi and P. Liatsis, "Co-evolutionary-based active contour models in tracking of moving obstacles", *Proc. International Conference on Advanced Driver Assistance Systems* (IEEE, London, 2001), pp. 58–62.
[17] L. A. MacEachern and T. Manku, "Genetic algorithms for active contour optimization", *Proc. IEEE Int. Sym. for Circuits and Systems* (IEEE Press, Piscataway, NJ, 1998), pp. 229–232.
[18] M.-S. Dao, F. G. B. De Natale, and A. Massa, "Edge Potential Functions (EPF) and Genetic Algorithms (GA) for Edge-Based Matching of Visual Objects", IEEE Trans. Multimedia **9**, 120–135 (2007).
[19] L. Ballerni and L. Bocchi, "Multiple Genetic Snakes for Bone Segmentation", in: Proc. EvoWorkshops, Lect. Notes Comput. Sci. **2611**, 346–356 (2003).
[20] R. C. Gonzalez and R. E. Woods, *Digital Image Processing* (Addison Wesley, Reading, MA, 1993), pp. 447–455.
[21] M. Srinivas and L. M. Patnaik, "Adaptive probabilities of crossover and mutation in genetic algorithms", IEEE Trans. Syst. Man Cybern. **24**, 656–667 (1994).
[22] OFFIS Institute for Information Technology website, http://www.offis.de/index-e.php/, accessed October 2006.
[23] A. P. Zijdenbos, B. M. Dawant, R. A. Margolin, and A. C. Palmer, "Morphometric analysis of white matter lesions in MR images: Method and validation", IEEE Trans. Med. Imaging **13**, 716–724 (1994).